AD-A141 832   THEORY OF LASER-INDUCED SURFACE CHEMISTRY WITH   1/1
           APPLICATIONS TO MICROELECT..(U) ROCHESTER UNIV NY DEPT
           OF CHEMISTRY   J T LIN ET AL. MAY 84
UNCLASSIFIED   UROCHESTER/DC/84/TR-51 N00014-80-C-0472   F/G 7/4   NL

END
DATE
FILMED
7-84
DTIC

MICROCOPY RESOLUTION TEST CHART

NATIONAL BUREAU OF STANDARDS 196 A

OFFICE OF NAVAL RESEARCH

Contract N00014-80-C-0472

Task No. NR 056-749

TECHNICAL REPORT No. 51

Theory of Laser-Induced Surface Chemistry with Applications
to Microelectronics and Heterogeneous Catalysis

by

Jui-teng Liu, William C Murphy and Thomas F. George

Prepared for Publication

in

I & EC Product Research and Development

Department of Chemistry
University of Rochester
Rochester, New York   14627

May 1984

DTIC
SELECTED
JUN 0 7 1984
E

84 06 06 009

AD-A141 832

DTIC FILE COPY

REPORT DOCUMENTATION PAGE		READ INSTRUCTIONS BEFORE COMPLETING FORM
1. REPORT NUMBER UROCHESTER/DC/84/TR-51	2. GOVT ACCESSION NO. HD-A141832	3. RECIPIENT'S CATALOG NUMBER
4. TITLE (and Subtitle) Theory of Laser-Induced Surface Chemistry with Applications to Microelectronics and Heterogeneous Catalysis		5. TYPE OF REPORT & PERIOD COVERED
		6. PERFORMING ORG. REPORT NUMBER
7. AUTHOR(s) Jui-tenq Lin, William C. Murphy and Thomas F. George		8. CONTRACT OR GRANT NUMBER(s) N00014-80-C-0472
9. PERFORMING ORGANIZATION NAME AND ADDRESS Department of Chemistry University of Rochester Rochester, New York 14627		10. PROGRAM ELEMENT, PROJECT, TASK AREA & WORK UNIT NUMBERS NR 056-749
11. CONTROLLING OFFICE NAME AND ADDRESS Office of Naval Research Chemistry Program Code 472 Arlington, Virginia 22217		12. REPORT DATE May 1984
		13. NUMBER OF PAGES 53
14. MONITORING AGENCY NAME & ADDRESS(If different from Controlling Office)		15. SECURITY CLASS. (of this report)
		15a. DECLASSIFICATION DOWNGRADING SCHEDULE

16. DISTRIBUTION STATEMENT (of this Report)

This document has been approved for public release and sale; its distribution is unlimited.

17. DISTRIBUTION STATEMENT (of the abstract entered in Block 20, If different from Report)

18. SUPPLEMENTARY NOTES

Prepared for publication in I & EC Product Research and Development

19. KEY WORDS (Continue on reverse side if necessary and identify by block number)

REVIEW ARTICLE	MIGRATION
LASER-INDUCED SURFACE CHEMISTRY	DESORPTION
MICROELECTRONICS	CHEMICAL REACTIONS
HETEROGENEOUS CATALYSIS	LITHOGRAPHY
ADSORPTION	ANNEALING

20. ABSTRACT (Continue on reverse side if necessary and identify by block number)

Theory and experiments are reviewed for how laser radiation can stimulate various component mechanisms which contribute to the complex chemistry involved in heterogeneous catalysis. These mechanisms include the processes of adsorption, desorption, migration and chemical reactions at a gas-solid interface. Applications of laser-induced surface chemistry to microelectronics in circuit deposition, lithography, annealing and final testing of the circuit are discussed. In addition to the review, some new theory is presented.

DD FORM 1473
1 JAN 73

THEORY OF LASER-INDUCED SURFACE CHEMISTRY WITH APPLICATIONS
TO MICROELECTRONICS AND HETEROGENEOUS CATALYSIS

Jui-teng Lin
Laser Physics Branch
Optical Sciences Division
Naval Research Laboratory
Washington, D.C.   20375

William C. Murphy and Thomas F. George
Department of Chemistry
University of Rochester
Rochester, New York   14627

Abstract

Theory and experiments are reviewed for how laser radiation can
stimulate various component mechanisms which contribute to the complex
chemistry involved in heterogeneous catalysis. These mechanisms include
the processes of desorption, migration and chemical reactions at a gas-
solid interface. Applications of laser-induced surface chemistry to
microelectronics in circuit deposition, lithography, annealing and final
testing of the circuit are discussed. In addition to the review, some
new theory is presented.

I. Introduction

During the past several years, the area of laser-induced surface chemistry has become an established interdisciplinary pursuit among researchers from the fields of physical chemistry, surface science and optics. A variety of interesting processes can be induced or modified at a gas-solid interface by laser radiation. These include desorption, migration and chemical reactions. Such processes are vital constituents of heterogeneous catalysis, and in Section II we shall review some of the key theoretical and experimental developments along these lines. Related laser-induced processes which have received attention are deposition, lithography and annealing. These are of prime interest in the microelectronics industry for use in the construction of integrated circuits, and in Section III we shall summarize the current state of the art and possible extensions. Concluding remarks are made in Section IV.

II. Heterogeneous Catalysis

Heterogeneous catalytic reactions involving fundamental gas-surface interactions at the phase interface are usually characterized by the following sequence of events:[1,2]

(1) Diffusional transfer of gas species (reactants) to the surface.

(2) Adsorption of reactants onto the surface.

(3) Events on the surface, e.g., migration, scattering and reaction.

(4) Desorption of products from the surface.

(5) Diffusion of desorbed species away from the surface.

The diffusion steps 1 and 5 are fairly well understood within a framework such as gas kinetic theory and generally do not play a critical role in the surface rate processes. Steps 2,3 and 4 involving the actual gas-surface interaction are usually the rate-determining steps and may be greatly influenced by laser radiation through the effects such as: (i) dissociation/decomposition of the reactants both in the gas phase and in an adsorbed phase; (ii) local heating of the substrate; (iii) selective excitation of the active mode of the adspecies; and (iv) bond breaking of the adspecies-surface complex through direct and indirect channels.

In this section, we shall first discuss the possible effects of laser radiation on the main steps in the heterogeneous catalytic reaction, namely, adsorption, migration and desorption (Parts A-C). The influence of laser radiation on the overall chemical reactions involving the combination of these individual steps will then be addressed in Part D.

A. Adsorption

When gaseous species (reactants) diffuse to a catalytic surface, collisions between these species and the surface will lead to adsorption,

either physically or chemically depending upon the forces responsible for the adsorption process. In physisorption, the electron cloud of the adspecies interacts as a whole with minimal distortion with the adsorbent. In chemisorption, on the other hand, the shape of the electron cloud is distorted and charge is interchanged with the adsorbent. In general, physisorption is a weaker bound state and involves higher mobility compared with the chemisorption. Physisorbed bonds are typically on the order of 10 kJ/mol, whereas chemisorbed are on the order to 100 kJ/mol or higher. The rate of adsorption can be limited by transfer phenomena such as:[1]

(1) The rate of mass transfer of the gas to the adsorbent surface.

(2) The rate of transfer of heat liberated by the adsorption process from the captured molecule to the adsorbent, and vice versa.

(3) The rate of surface migration along the surface of the adsorbent to the most favorable adsorption site.

Therefore, a complete description of adsorption kinetics includes not only the time variation of the total amount adsorbed, but also the relationship among the adsorption rate, pressure and substrate temperature.

The influence of laser radiation on the aforementioned adsorption kinetics may be thermal or nonthermal depending upon the frequency of the radiation and the state of the excited species (gas or adsorbed phase). Adsorption, either physisorbed or chemisorbed, may be enhanced by laser radiation in a variety of ways, such as photodissociation of the reactants, vibrational excitation of the gas-phase species, electronic excitation and/or electron-hole generation of the adsorbate-adsorbent complex, and direct local heating of the substrate. Experimental studies of laser-enhanced adsorption have been extensively explored, and reported examples are: (i) multiphoton dissociated SF_6 adsorbed on Si surface;[3] (ii) dissociation of N_2 molecule

which otherwise cannot chemisorb on metal surfaces such as Cu and Ru;[4] (iii) single-photon photolyzed Br_2 interaction with Ge;[5] (iv) vibrational excitation of methane as part of the chemisorption mechanism on metal surfaces.[6,7]

Theories of gas-surface scattering and sticking processes in the absence of laser radiation have been presented in the past several years.[8] It is known that the incoming particle can be adsorbed when its kinetic energy is dissipated into the other degree of freedom, e.g., excitation of phonons and electron-hole generation. The rate of adsorption may be described by[1]

$$k_A = s\phi \exp(-E_A/k_B T), \tag{1}$$

where s is the sticking probability of the incoming particles with flux ϕ, E_A is the activation energy, and k_B is Boltzmann's constant. In the presence of laser radiation, the adsorption rate may be enhanced via two channels: either increasing the sticking probability or overcoming the adsorption barrier. The effective activation energy may be lowered by the absorption of photon energy $\hbar\omega$, i.e., $E_{eff} = E_A - \hbar\omega$, which enhances the rate of adsorption.

To demonstrate the influence of laser radiation on the transition of the incoming particle from a continuum to a bound state, let us first discuss the energy transfer involved in an inelastic scattering process. The energy transfer from the incoming particle to the substrate via surface excitations (phonons or electron-hole pairs) is given by the Fourier transform of the driving force acting on the substrate surface,[9]

$$\Delta E_0 = \frac{1}{2m} |\int_{-\infty}^{\infty} dt\, e^{-i\omega_0 t} F(t)|^2, \tag{2}$$

for systems in which the surface excitations are not damped. Here m is the mass of the substrate atom, and ω_0 is the frequency of the particle-substrate

bond. The driving force is for a fixed normal distance z of the incoming
particle from the substrate is given by $F(t) = -\partial V(t)/\partial \underline{x}$, where $V(t)$ is the
dynamical potential between the particle and the susbstate, and $\underline{x}$ is the posi-
tion vector of the substrate atoms. In general, the surface excitations are
coupled to the bulk phonons which give rise to a damping factor Γ in the
equations of motion for $\underline{x}$. These phonons or excited bosons have a frequency
distribution $\rho(\omega)$, and the overall energy transfer is then given by

$$\Delta E = \int_{-\infty}^{\infty} d\omega \int_{0}^{t_c} dt \, \rho(\omega) F(t,\omega) \underline{\dot{x}}(t,\omega), \tag{3}$$

where F now has a frequency dependence for the excited bosons, and t_c is the
collision time. The velocity $\underline{\dot{x}}$ of the excited bosons can be found in terms
of the solution to the damped equations of motion

$$\underline{\ddot{x}} + 2\Gamma\underline{\dot{x}} + \omega^2\underline{x} = F(t)/m. \tag{4}$$

Laser radiation can influence the adsorption of the species or the energy
transfer dynamics through the driving force, for example, by increasing the
collision time t_c.

To further demonstrate these effects, we consider a semiclassical model
as shown in Figure 1. The probability of the incoming particle to make a
transition from state I to II' and to adsorb onto the surface may be given by
a Golden-Rule-type expression,

$$P_{I,II'} = \sum_{j} \int_{-\infty}^{\infty} d\omega_j \, P_1 P_2 P_3(\omega_j), \tag{5}$$

where P_1 is the probability of an electronic transition from state II to II',
P_2 is the Landau-Zener-type curve-crossing probability from state I to II',
and $P_3(\omega_j)$ is the probability for the excitation of the j-th phonon, or electron-
hole pair, with energy $K_j - \hbar\omega_j$ and density of states $\rho(\omega_j)$, where K_j is the
initial kinetic energy. The overall sticking probability or transition
probability $P_{I,II'}$ can be enhanced by laser radiation via two channels:[10]
(i) electronic excitation of the adspecies potential, i.e., the transition
probability P_1; and (ii) vibrational excitation within the electronically
excited state II', which compensates the energy mismatch $K_j - \hbar\omega_j$ and in turn
increases the diabatic curve-crossing probability P_2 and the energy transfer
probability P_3 via the surface excitations. We note that the energy transfer
probability P_3 is proportional to t_c^2, which must be larger than the inverse of
the "predissociation broadening" in order that the incoming particle may be
significantly trapped in the surface potential well. We also note that laser-
enhanced adsorption in general is accompanied by the other surface processes
such as migration and desorption. For example, in pressure-limited adsorption,
the adsorption rate of the reactants is limited by the co-adsorption of the
products. Laser desorption of these products will open the product-limited
channel and enhance the adsorption of the reactants. This will be discussed
further in Part D where we study the influence of laser radiation on the
overall reaction.

B. Migration

We shall now investigate the influence of laser radiation on the third
step, migration, which follows the second step, adsorption. In many cases,
adspecies in the vibrational ground state of the surface potential, such as
shown by curve II in Figure 1, are unable to migrate along the surface,

particularly for chemisorbed species whose migration barrier is higher than the thermal energy provided by the substrate. In these situations, the laser is essential to inducing migration, which may be achieved via several channels:

(1) Local laser heating of the substrate with thermal energy sufficiently high enough to overcome the migration barrier.

(2) Vibrational excitation of the adspecies followed by a transition from a strongly chemisorbed state to a mobile physisorbed state.

(3) Electronic excitation of the adspecies-surface complex causing the rearrangement of the molecular bond structure.

In channel (1), the migration may be followed by a desorption process if the substrate surface is further heated. Channel (2) may also be assisted by channel (1) through indirect heating of the substrate, where the substrate phonons are strongly coupled to the active mode of the adspecies. Finally, laser-induced decomposition and/or predissociation of the admolecule are usually involved in channels (2) and (3), where the dissociated adspecies encounters a lower migration barrier compared with that of the associated adspecies.

Experimentally, little work has been done on laser-induced migration.[11] In the following discussion, we shall look at the theoretical aspect and focus on one of the most significant migration channels, namely the vibrational excitation of the adspecies. The dynamics of laser-induced migration may be well described by a microscopic Hamiltonian,[12]

$$H(t) = H_0(Q_1, Q_2, ..., Q_N) + \sum_{k,k'} [V_{kk'}(Q_1, Q_2, ..., Q_N) + H_{AF}(t)] c_k^\dagger c_{k'}, \qquad (6)$$

where H_0 is the unperturbed Hamiltonian of the system (adspecies plus sub-strate), with N normal coordinates Q_j, $V_{kk'}$ is the lattice-site-dependent interaction potential of the adspecies, c_k^+ and $c_{k'}$ are the site operators for a transition from k-site to k'-site, and $H_{AF}(t)$ is the interaction Hamiltonian between the laser field and the active mode. It is seen that, from Eq. (6), migration or lattice-site-hopping of the adspecies may be achieved by both the thermal phonon fluctuations, through $V_{kk'}$, and the coherent laser excitation, through H_{AF}.

A second-quantization representation of the above dynamic Hamiltonian enables us to calculate the migration rate, which is characterized by the Fourier transform of the autocorrelation function of the interaction Hamiltonian. Employing the density matrix technique, we obtain a generalized master equation (GME) of the form[13]

$$\frac{dP(m,n,i,t)}{dt} = \int_0^t dt' \sum_{m',n',i'} [W_{mm',nn'}^{ii'}(t-t')P(m',n',i',t') - W_{m'n,n'n}^{i'i}(t-t')P(m,n,i,t')], \tag{7}$$

where $P(n,n,i,t)$ is the probability of finding the adspecies at the lattice site (m,n) and at the i-th vibrational level at time t, $W_{mm',nn'}^{ii'}(t)$ is a time-dependent transition rate from state (m',n',i') to (m,n,i), and $W_{m'm,n'n}^{i'i}(t)$ is the associated reverse rate. We note that in the above general form the transition rates are not only time dependent but are also governed by both the site c coordinates (m,n) and the vibrational states of the adspecies (i) which are activated by the laser radiation.

Depending on the migration barrier and the vibrational spectrum and status (physisorbed or chemisorbed) of the adspecies, laser radiation may

induce two types of migration: horizontal migration for a transition from (m,n,i) to (m',n',i) and oblique migration for a transition from (m,n,i) to $(m',n'i')$ with $i' \geq i$. The first type usually involves a physisorbed state of highly mobile adspecies and may be thermally induced either by direct laser heating or phonon-mediated excitation. The transition or migration rate of this type may be described by an Arrhenius form

$$k_1 = k_0 \exp[-E_M/k_B(T_0 + T_L)] \tag{8}$$

where E_M is the migration barrier, and T_L is the laser-induced temperature rise of the substrate whose initial temperature is T_0. The second type of migration, on the other hand, may be written as

$$k_2 = k_0' \exp[-(E_M - <n>\hbar\omega)/k_B T_0]. \tag{9}$$

Here the effective migration barrier is reduced by the amount of photon energy absorbed by the adspecies, $<n>\hbar\omega$, where $<n>$ is the average number of photon absorbed. T_L does not appear in Eq. (9) since the substrate is not significantly heated, i.e., $T_L \ll T_0$.

In the Markoffian or random-phase approximation and within the assumption of only nearest-neighbor hopping, the above GME reduces to the standard master equation (ME). On the supposition that the migration barrier is lower in one particular direction, then the adspecies will migrate preferentially in this specific direction, and the 2D ME further reduces to a 1D ME,

$$\frac{dP_n}{dt} = W[P_{n+1} + P_{n-1} - 2P_n], \tag{10}$$

where P_n is the probability associated with the n-th lattice site in this preferred direction. The associated root-mean-square displacement may be calculated from the above ME, and the migration coefficient is thus found to be[14,15]

$$D = 2(W_T + W_L + W_I)d^2, \tag{11}$$

where d is the lattice-site spacing, and $W_{T,L,I}$ are the migration rates caused, respectively, by the thermal phonons, laser radiation and their interference. The thermal excitation rate is given by

$$W_T = W_0 \exp(-E_M/k_B T_s), \tag{12}$$

which is an Arrhenius form as usual. However, the laser excitation rate is given by a Lorentzian

$$W_L = AI/(\Delta^2 + \Gamma^2), \tag{13}$$

where A is proportional to the square of the derivative of the transition dipole of the adspecies, I is the laser intensity, and Δ and Γ are the detuning and the damping factors, respectively. The salient feature of the laser excitation rate is that selective migration, either spatially-selective or adspecies-selective (for a single isotope or isotopic mixture), may be achieved by tuning the laser frequency to meet the resonance condition $\Delta \approx 0$. For small values of Γ, the adspecies of interest may be excited without significantly heating the substrate. Application of laser-induced migration to diffusion-limited rate processes will be discussed in Part D.

C. Desorption

Desorption of adspecies from a solid surface may be achieved by conventional thermal/flash processes,[16] electron-stimulated processes,[17] and laser-stimulated processes which will be discussed in this part of Section II. Desorption processes stimulated by UV, visible and IR laser radiation have been studied extensively in the past several years both experimentally[18] and theoretically.[19] Examples of UV/visible-laser-induced desorption involving the electronic excitation of the adspecies are: (i) desorption of CO from metal surfaces;[20] (ii) desorption of CO_2 from metal oxide surfaces;[21] and (iii) desorption of molecular ions from molecular crystal surfaces.[22] Examples of experimental studies of IR-laser-induced desorption involving resonant vibrational excitation of the admolecule are also available: (i) desorption of CH_3F from NaCl film deposited on a single NaCl crystal;[23] (ii) desorption of CO from Pd surface;[24] and (iii) desorption of pyridine from KCl, Ag island film/quartz, Ag(110) and Ni foils.[25] Another type of desorption process, namely laser-induced thermal desorption, has been reported. Examples are: (i) desorption of D_2 from W surface covered by D atoms using a Q-switch Nd:glass laser;[26] (ii) desorption of CO from Fe(110) and Cu(100) surfaces.[11,27]

Selective laser-stimulated desorption achieved by IR radiation is the most widely studied. We shall therefore discuss possible mechanisms for this type of desorption and compare the theories which are available. Laser-desorption may be achieved by one or more sequential channels which, as shown in Figure 2, are cataloged into six types.[19] For type I processes involving multiphoton excitation of the adspecies, calculations have been reported based on harmonic potential,[28] anharmonic potential[29] and Morse potential[30] models.

In the Morse potential model, the calculated laser intensity for desportion is unlikely higher than one would expect. Therefore, the concept of a "quasicontinuum" is introduced in type II. Within the quasicontinuum regime, the resonance condition is always satisfied and photon energy may be deposited into the adspecies to cause bond breaking without being blocked by the anharmonicity. Indirect desorption via Fano-type bound-continuum coupling is also possible as shown in type III. Calculations based on this type of desorption channel and using the master equation technique have been investigated.[31,32] For an adspecies which is strongly coupled to the substrate by a highly anharmonic surface potential, the desorption channel might be assisted by thermal phonons as shown in types IV and V. Another indirect desorption, type VI, is accompanied by other rate processes such as migration, scattering, recombination and dissociation of the reactants or the products.

We shall mention as an example the simple theory involved in the most favorable desorption channel, type V. When the adspecies is highly excited into the quasicontinuum and in thermal equilibrium with the locally-heated substrate, the desorption rate may be approximated by[19]

$$k_D = k_0 \exp[-(E^* - \hbar\omega \langle n \rangle)/k_B T_S^*],\qquad(14)$$

where E^* is the threshold desorption energy, T_S^* is the maximum surface temperature at the adsorption site, and $\langle n \rangle$ is the average number of photons adsorbed by the adspecies. We note that for systems with high coverage, $\theta > 0.5$, the interactions among the adspecies may be significant and the desorption energy should be modified as $E^* + \beta\theta$, where $\beta\theta > 0$ is the correction factor (assumed to be linearly proportional to the coverage).

D. Chemical Reactions

We have so far discussed laser-stimulated dynamics, adsorption, migration and desorption. In general, laser-stimulated surface processes (LSSP) should include (in addition to the above three processes) recombination, decomposition, deposition, etching, and annealing, etc. Before investigating the influence of laser radiation on the overall surface rate processes, some of the important features of LSSP and their applications and implications to surface chemistry/physics are summmarized as follows:[19]

(1) Enhancement of surface diffusion-limited reactions.

(2) Enhancement of the mobilities of selective species in a multicomponent environment.

(3) Control of the concentration of reagents by selective desorption or excitation-induced migration of the species.

(4) Study of decomposition and recombination rate processes on solid surfaces.

(5) Study of the catalytic properties and heterogeneity features of the adsorbents.

(6) Isotope separation and mass separation of adspecies via selective desorption (laser chromatography).

(7) Study of the composition and location of the active sites and the conformation structure of the adspecies.

(8) Fabrication of microelectronics via laser-induced chemical vapor deposition, microetching and laser annealing.

Laser radiation may influence overall surface chemical reactions in a variety of ways depending upon the physical and chemical states of the excited species and frequency spectra of the adspecies-surface system. We shall focus on

vibrational-excitation-enhanced reactions and diffusion-limited processes. Prototypes of heterogeneous rate processes are (where K denotes the catalytic substrate):

(i) Excitation of a reactant in the gas phase.

$$A + K \rightarrow A/K \begin{cases} \rightarrow AK + K & \text{(a)} \\ \rightarrow B + C + K & \text{(b)} \end{cases}$$
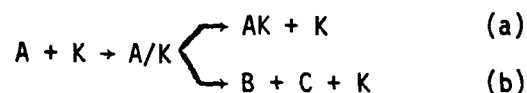
(ii) Excitation of an intermediate adsorbed on the surface.

$$(A + B)/K \xrightarrow{\ k_1\ } (AB)/K \xrightarrow{\ k_2\ } \begin{cases} \dashrightarrow AB + K & \text{(c)} \\ \dashrightarrow C + D + K & \text{(d)} \end{cases}$$
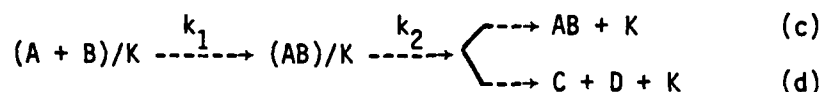
In (i), laser radiation may enhance the adspecies-substrate reaction (a) and the decomposition process (b) catalyzed by the substrate. Examples of reaction (b) are the decomposition of CH_4 on Rh[33] and HCOOH on Pt.[34] An example of reaction (a) is IR-laser-induced microetching of Si in the SF_6/Si system.[25]

In (ii), laser radiation may influence the overall reaction rate in several ways: (1) by increasing the mobility of the reactant atoms (A or B) through photon excitation of the A-K or B-K bond with subsequent enhancement of the reaction rate k_1 [see type (VI) in Figure 2]; (2) by removal of the excess energy from the unstable complex (AB) on the substrate surface via laser-stimulated emission accompanied by surface-phonon-mediated relaxation, thereby increasing the reaction rate k_2; (3) by breaking the AB-K bond either directly through laser excitation of the adspecies or indirectly through thermal desorption by laser heating of the surface [see types (I) and (IV) in Figure 2]; and (4) by desorption of the products, thereby increasing the reaction rate k_2 in (d). We shall first look at the influence of laser

radiation on reaction (d) and then consider reaction (c) through laser-enhanced migration of the reactants.

Let us consider a decomposition reaction whose rate is inhibited by the products. Examples of this type of decomposition kinetics are: (i) N_2O on Pt where the rate of decomposition is inhibited by the adsorbed oxygen; (ii) ammonia on Pt whose decomposition rate is greatly inhibited by the hydrogen formed on the surface; and (iii) the dehydration of ethyl alcohol on aluminium oxide. For simplicity we shall consider processes where only one product (B) is co-adsorbed with the reactant (A). According to Langmuir's theory, the coverage of the reactant, θ_A, and the coverage of the product, θ_B, are given by[35]

$$\theta_A = \frac{Kp_A}{1+Kp_A+K'p_B} , \qquad \theta_B = \frac{K'p_B}{1+Kp_A+K'p_B} , \tag{15}$$

where $K = k_1/k_2$ and $K' = k_1'k_2'$ are the equilibrium constants of adsorption, $k_1(k_1')$ and $k_2(k_2')$ are the adsorption and desorption rate constants for the reactant (product), and $p_{A,B}$ are the partial pressures of the reactant (A) and product (B). For first-order kinetics, the chemical reaction is described by

$$\frac{dx}{dt} = k\theta_A , \tag{16}$$

which is proportional to the coverage of the reactant. Therefore, the reaction rate may be greatly enhanced by increasing the reactant coverage which, as shown in Eq. (15), is inhibited by the product coverage, or $K'p_B$. To demonstrate the influence of laser desorption of the product on the reactant coverage,[36] let us rewrite Eq. (15) as

$$\theta_A = \frac{Kp_A(1-\theta_B)}{1+Kp_A} .$$

(17)

It is seen that the decrease of θ_B will increase θ_A, i.e., enhancement of the reactant coverage, and hence the reaction rate, may be achieved by laser-induced selective desorption of the product.

We shall now investigate the influence of laser radiation on a Langmuir-Hinshelwood process whose reaction rate is limited by the diffusion (or migration) of the reactants on the catalytic surface. Considering the surface reaction $A + B \rightarrow AB$, with the assumption that B is fixed and A is diffusing toward it, the probability of finding A at some position r at time t is given by a diffusion equation[37]

$$\frac{\partial P(r,t)}{\partial t} = D\nabla^2 P(r,t) + J - \frac{P(r,t)}{\tau} ,$$

(18)

where D is the diffusivity of A with a resident time τ and flux J onto the surface. Employing standard techniques, we can find the steady-state two-dimensional solution of Eq. (18) under two conditions: $P(r_A,t) = 0$ and $P(r_0,t) = $ constant, where r_A is a critical distance for the reaction to occur and r_0 defines the initial concentration of A molecules. For the situation of very long residence time, i.e., $D\tau \rightarrow \infty$, the steady-state rate constant is given by[38]

$$k = 2\pi D/\ln(r_0/r_A).$$

(19)

In the presence of laser radiation which selectively induces the migration of adspecies A, the total diffusivity consists of two components (we are ignoring the interference term),

$$D = D_T + D_L, \tag{20}$$

where the thermal part is given by an Arrhenius expression

$$D_T = D_0 (\frac{\pi}{4k_B T E_A})^{1/2} e^{-E_A/k_B T}, \tag{21}$$

where E_A is the activation energy of migration. The laser-induced component is given by

$$D_L = D_0' I / (\Delta^2 + \Gamma^2), \tag{22}$$

where I is the laser intensity, and Δ and Γ are the detuning and damping factors, respectively, of the excited admolecule A. We have thus seen that the rate constant of a diffusion-limited reaction may be greatly enhanced by laser-induced migration of the reactants (A or B). The unique feature of laser-induced migration is characterized by the frequency-sensitive expression of D_L, which enables us to selectively enhance the desired reaction channel while without perturbing the remaining environment. A possible application of laser-induced migration is diffusion-controlled isotope separation on a solid surface, which might not be possible when the reactants are in gas phase.[39] Other types of laser-enhanced surface rate processes,[40] such as laser-controlled gas diffusion through a porous membrane[41] and rate processes on metal surfaces involving electronic excitations,[42] have been reported.

III. Microelectronics

In the creation of integrated circuits (IC), the processes discussed in Section II all play an important role. For instance, the desorption process is necessary to initially clean the substrate, and the migration process can be used to move dopants to a desired site. However, whereas catalysis takes place on a surface, the creation of microelectronic circuits on a semiconductor chip involves the transformation of the surface into zones of different electrical properties.

In the following parts of this section, we focus on the major steps in the fabrication of IC and the role the laser can play in such processes. In Part A we examine how the rate and position of deposition can be controlled with a laser. In Part B we show that the continuation of the deposition process can be used to create periodic patterns on surfaces, which in turn can be a means to construct highly-ordered IC chips. Finally, in Part C, we discuss how the laser can be used in the last stages of circuit preparation.

A. Deposition

To control the deposition process, a laser can be used to effect changes on the substrate surface or on the adspecies. In regard to the adspecies, laser-induced chemical vapor deposition (LCVD) may be cataloged into: (i) photo-lytic processes where the reactant gas molecule is dissociated (or decomposed) by the laser radiation in the region near the substrate surface, and (ii) pyro-lytic processes where the reactant is thermally decomposed when it is adsorbed on the substrate.[43] The experimental aspects of LCVD have been extensively reviewed,[18b,44] and we shall present some of the theoretical aspects below.

A two-step model of LCVD has been proposed by Ehrlich et al[45] to describe experiments where metal atoms obtained from gaseous organometallic compounds are deposited on a semiconductor. In this model, the initial deposition is achieved by pyrolytic decomposition of the adsorbed organometallic to form the metal atoms and then followed by gas-phase photolytic decomposition to form the bulk of the deposition. Experimental evidence has demonstrated that the gas-phase decomposition is the dominant factor in a specific system.[46] In general, both photolysis and pyrolysis should contribute to LCVD, so that it is therefore desirable to develop some relationship among the deposition rate, laser parameters such as intensity and beam radius, pressure of the reactants and temperature of the substrate.

We first consider the pyrolytic processes. The deposition rate achieved by laser-induced decomposition of the adsorbed species is given by

$$R_1 = \theta \sigma_A I^m / \hbar \omega, \tag{23}$$

where σ_A is the decomposition cross section of the adspecies with coverage θ, I is the laser intensity with frequency ω, and m is a power-law factor $(1/3 \leq m \leq 1)$. For a square pulse with a focused beam radius of α on the substrate, Eq. (23) may be expressed in terms of the laser power defined by $P_L = \pi \alpha^2 I$, which leads to the power-law expression

$$R_1 = C_1 \alpha^{-2m}. \tag{24}$$

For photolytic processes, on the other hand, the deposition rate governed by dissociation, diffusion and sticking of the gas species is given by

$$R_2 = s N_g \alpha \sigma_g I^{m'} / \hbar \omega, \tag{25}$$

where s is the stricking probability of the photodissociated species, with cross section σ_g and concentration N_g, and m' is another power-law factor. Here we have assumed that the deposition is formed by those species which are within the distance α from the substrate surface. Similar to Eq. (24), Eq. (25) may also be expressed as a power-law,

$$R_2 = C_2 \alpha^{-(2m'-1)}. \tag{26}$$

Eqs. (24) and (26) provide an important criterion for separating the photolysis and the pyrolysis involved in LCVD via the parameters m and m'. Note that even when m = m', the power law of R_2 is quite different from that of R_1. For example, in a UV deposition of organometallic gases, measurements show that $R = c\alpha^{-n}$ with n = 0.73, which indicates that the photolytic process is dominant.[46] These experimental results may be well fitted by Eq. (26) with m' ≈ 0.87. We note that an oversimplified model with the assumption of linear absorption, i.e., m = m' = 1 giving $R_1 = c_1 \alpha^{-2}$ and $R_2 = c_2 \alpha^{-1}$, does not provide a power law consistent with the measurement.[46] It is more likely that m > m' and m',m < 1, given the assumption that both multiphoton processes and phonon relaxation are involved in the pyrolysis and the photolysis.

Mass-transport limitations on the rate of LCVD have also been reported.[44,47] Two kinetic regimes have been proposed: (i) the surface kinetic regime where the deposition rate is proportional to the reactant pressure when the laser beam radius, α, is smaller than a scaling length, α_0, and (ii) the diffusion-limited regime, $\alpha \gg \alpha_0$, where the deposition rate is limited by the diffusion kinetics and is independent of pressure.

Experiments have also shown that due to the nonlinear dependence of the deposition rate on temperature, the resulting LCVD linewidth (via pyrolytic processes) may be substantially narrower than both the surface

temperature and the laser beam spatial profiles.[44,48,49] Generation of micro-scale LCVD via pyrolysis may be analyzed by an overall reaction rate which is governed by the rate-limiting steps, namely, the decomposition of the adsorbed reactants and desorption of the product gas from the substrate. To demonstrate the spatial resolution of LCVD, let us consider the Arrhenius-type reaction rate

$$R(r) = R_0 \exp[-E_A/k_B T^*(r)], \tag{27}$$

where E_A is an activation energy (for the deposition) and $T^*(r)$ is the peak surface temperature of the laser-heated substrate. Let us assume a Gaussian laser profile, both temporally (in t) and spatially (in r):

$$I(t,r) = I_0 \exp[-(r/\alpha)^2 + (t/t_p)^2]. \tag{28}$$

We may then write[50]

$$T^*(r) = T_0 \exp(-r^2/\alpha^2), \tag{29}$$

$$T_0 \approx 0.8\, T_s(t_p,0). \tag{30}$$

$T_s(t_p,0)$ is the peak surface temperature at the spot center of a square (temporal) laser, with pulse width t_p, given by

$$T_s(t_p,0) = 2I_0(t_p/\pi K\rho C_V)^{1/2} \tag{31}$$

where K is the thermal conductivity, ρ is the mass density, and C_V is the heat capacity.

Combining Eqs. (27) and (28), we may evaluate a spatial scaling factor S defined by the ratio of the e^{-1} fall point width of the temperature (or laser intensity) profile (2α) and of the deposition profile $(2W)$,

$$S = [\tfrac{1}{2} \ln(1+k_B T_0/E_A)]^{-1}$$

$$\simeq 2E_A/k_B T_0, \qquad \text{for } k_B T_0 << E_A. \tag{32}$$

As shown in Figure 3, the scaling factor is an increasing function of E_A for a fixed surface temperature, and the LCVD spatial profile may be significantly narrower than that of the temperature (or intensity). Experimental results have demonstrated $S \simeq 2.5$ for Ni deposited on a silica surface with a focused CO_2 laser[48] and $S \simeq 5$ for a diffusion-limited submicrometer B doping pattern.[49]

In addition to the above processes, we can also effect changes in the deposition process by using the laser to excite the surface of the substrate. To do this, we must first consider the energy level structure of the surface. In a crystalline solid, the electronic energy levels form a number of quasi-continuous valence and conduction bands. In a semiconductor, the upper valence band and lower conduction band are separated by an energy gap; in a metal these bands overlap. The electronic charge density associated with these energy bands is more or less uniform throughout the crystal. With the addition of a surface, however, a number of extra bands and local states are formed.[51] Futhermore, the charge density associated with these surface bands is localized in the surface region. Consequently, by using a laser to excite electrons to or from these surface bands, the surface charge density could be increased or decreased. Using a simple one-dimensional (1-D) model, we shall show that this process and the subsequent Coulombic interaction with an dopant adspecies could enhance the deposition process. Furthermore, by selective excitations, the laser can be used to control the type and position of the deposited species.

For a 1-D semiconductor of length L and lattice constant a, the solutions of the Schrödinger equation can be obtained within the nearly-free-electron approximation. The energy for the bulk electronic states is

$$E_k = \frac{1}{4}\left\{[k^2 + (k-g)^2] \pm \sqrt{[k^2 - (k-g)^2]^2 + 4E_g^2}\right\} \,, \tag{33}$$

where E_g is the band gap energy, k is the wavenumber of the electron, and $g = 2\pi/a$ is the reciprocal lattice vector. The results for the conduction band (positive branch) and the valence band (negative branch) are illustrated in Figure 4. The wavefunctions are construction from sums of plane waves.[19a,51] For example, at the top of the valence band we have

$$\psi_k(z) = \frac{2}{L^{1/2}} \sin[(\tfrac{g}{2})(z - \tfrac{a}{2}) + \theta] \tag{34}$$

for inside the semiconductor and

$$\psi_k(z) = \frac{2}{L^{1/2}} e^{-q(z - \frac{a}{2})} \sin\theta \tag{35}$$

for outside the semiconductor. The phase factor, θ, is determined by the continuity condition and $q = (2W - k^2)^{1/2}$, where W is the sum of the work function and Fermi energy.

Since the semiconductor is finite, in addition to the above solutions of the Schrödinger equation, there exist solutions with complex crystal momentum:[52,53]

$$k = g/2 + i\kappa. \tag{36}$$

Using this in the energy expression, Eq. (33), we obtain

$$E_\kappa = \frac{1}{2}\left\{(\frac{g}{2})^2 - \kappa^2 \pm \sqrt{E_g^2 - \kappa^2 g^2}\right\}.$$ (37)

Lifewise, the nearly-free-electron approximation to the wavefunction gives

$$\psi_\kappa(z) = C_S \sin[(\frac{g}{2})(z - \frac{a}{2}) + \theta]e^{-\kappa(z - \frac{a}{2})},$$ (38)

where C_S is a normalization constant.[19a] The external wavefunction will have the same form as Eq. (35). The surface state energy, Eq. (38), is also illustrated in Figure 4 by the band labeled S. These are surface states since the charge density associated with them is localized in the surface region due to the exponential factor in Eq. (38). The bulk states, Eqs. (34) and (35), however, are not damped and thus have charge distributed throughout the system.

If we excite electrons from the valence band to the surface band, charge will be transfered from the bulk of the semiconductor to the surface. The resultant Coulombic effect could have significant influence on the deposition process. Laser-induced transitions to the surface states will be governed by the integral

$$H_{\kappa k}(t) = <\kappa|\vec{A}\cdot\vec{p}|k>,$$ (38)

where $\vec{A}$ is the vector potential of the laser radiation and $\vec{p}$ is the momentum operator of the electron. Using the appropriate wavefunctions in Eq. (38), it can be shown that the only appreciable bulk-to-surface transition occurs

when the real part of the crystal momentum is conserved. Since the surface state crystal momentum is given by Eq. (36), bulk states excited by the laser will be confined to the top of the valence band.

To calculate the transition rate, T, the square modulus of Eq. (38) is summed over all initial and final states. After some algebra, this gives[19a,54]

$$T = \frac{8\pi}{137} \frac{I_g^2 L}{E_g \omega^2} \frac{|<\kappa|\frac{d}{dz}|g/2>_0|^2}{1 - e^{2\kappa a}} |\frac{d\kappa}{dE_\kappa}|, \tag{39}$$

where I is the intensity of the laser, ω is the laser frequency in resonance with the transition, and the subscript zero indicates integration over the first unit cell. Finally, we obtain the cross section, σ, from the relationship,

$$\sigma \equiv \frac{\omega T}{I}. \tag{40}$$

Figure 5 depicts the behavior of the cross section over the entire frequency range. The values for the lattice constant, a = 2.35 Å, and the energy gap, E_g = 1.17 eV, are typical of silicon. At both extremes κ goes to zero and σ diverges. This occurs because at the surface band edge the charge associated with the surface states becomes more and more delocalized throughout the lattice, until at κ = 0 the charge is completely delocalized. At this point the surface states become bulk states, and instead of cross sections, one should consider absorption coefficients.

Since the charge depth increases as we move away from the mid-gap region, we wish to excite surface states near 0.5 E_g to obtain the greatest

effect on the surface charge. From Figure 5, we see that in this region
the cross section is quite substantial. Consequently, we would expect a
laser tuned to a frequency near 0.5 E_g to be an effective controller of
surface charge.

To examine the effect of this surface charge on adspecies, we have
evaluated the electronic densities in the surface region for silicon.[54-56]
The resultant densities exhibit oscillations due to the concentration of
charge around the ions. If one excites surface states near the gap center,
the charge concentration in the first few layers of the surface will
increase up to about thrice the average bulk density.

If a charged dopant is above the surface, this excess charge in the
surface region can produce a marked effect on the dopant-surface inter-
action. This interaction can be written classically as

$$U(z_I) = -\int d\vec{r} \; n(z) \; v(r), \tag{41}$$

with

$$r = [x^2 + y^2 + (z - z_I)^2]^{1/2}, \tag{42}$$

where $n(z)$ is the electron charge density and $v(r)$ is the electron-ion
potential of the adspecies at z_I. If we take $v(r)$ to be Coulombic with
Thomas-Fermi screening, we can readily evaluate the integrals over x and
y to obtain

$$U(z_I) = -\frac{2\pi Z}{\lambda} \int_{-\infty}^{\infty} dz \; n(z) e^{-\lambda|z-z_I|}, \tag{43}$$

where λ is the Thomas-Fermi screening parameter and Z is the charge on the adspecies. Since we are not concerned with the interaction of adspecies with the semiconductor in the ground state, we only consider the excited surface state contribution to the potential (superscript S). We can thus obtain

$$\frac{^S U(z_I)}{Z} = e^{-\lambda z}I_A(\kappa) - e^{-2qz}I_B(\kappa),\qquad(44)$$

where the coefficients $A(\kappa)$ and $B(\kappa)$ are given elsewhere.[19a] This equation has been evaluated for a number of surface states, and the results are plotted in Figure 6. As one moves to large $|\kappa|$ (energies near the gap center), the curves clearly show that both the magnitude and the range of the surface charge interaction increase. Since we have found that the surface charge also increases under these circumstances, this is exactly what is expected. All curves, however, show an appreciable contribution to the potential produced by the surface with $|\kappa| > 0.1\ E_g/g$.

Thus, we see that an appreciable effect on the dopant-surface interaction can be produced by use of a laser to localize electronic charge in the surface region. If the dopant of interest is positively charged, the rate of deposition can be controlled by the laser. Furthermore, negative species in the dopant gas will be repelled; thus the effect of impurities would be minimized. In a more complete model of a semiconductor, both occupied and empty surface states could exist in the ground state. A laser could then be used to excite holes as well as electrons to these surface states, and thus the deposition of both negatively and positively charged dopants could be controlled.

Although most IC technology involves the doping of semiconductor surfaces, metals still play an important role in microelectronics. The most obvious use, of course, is the use of metal interconnections for the circuits on a semiconductor chip. Since other layers may well be deposited on these metal connectors, laser control of the metal surface charge would also be beneficial in the deposition process.

As with a semiconductor, a metal can be modeled as a truncated 1-D chain with expressions for the bulk and surface wavefunctions and their associated energies of the same form as those for the semiconductor.[19a,57] However, whereas the lower band in a semiconductor is completely filled (see Figure 4), in a metal this band is only partially filled. For example, in the case of sodium, the top of the lower band lies at 3.8 eV, but the band is only occupied up to 3.1 eV in the ground state.

If we shine a laser on the metal, electrons cannot be directly excited from the bulk to the surface. This is due to our selection rule which says that we can only excite bulk states with $k = g/2$. In a metal, there are no occupied bulk states with real crystal momentum at or near this value. To overcome this problem, the electrons can be excited to the $k = g/2$ state with the phonons of the crystal before excitation into the surface states by the laser photons. Thus photons would supply the energy needed for the transition, and phonons would supply the needed crystal momentum.

If we assume a thermal distribution of phonons, the cross section for the excitation of surface electrons in a metal can be readily calculated:

$$\sigma = \frac{1}{N} \sum_{\kappa} S(k) \sigma^{(1)}(\kappa), \tag{45}$$

where N is the number of atoms in the metal, k is the wavevector of the desired phonon, and $S(k)$ is a scaling factor.[57] The cross sections, $\sigma^{(1)}(\kappa)$, are of the same form as those calculated for semiconductors, Eqs. (39) and (40). This cross section, given by Eq. (45), was calculated and found to be smaller than the semiconductor cross sections by a factor of 10^{-4}. This means that a larger laser power (10 - 100 kW/cm^2, in contrast to 1 - 10 W/cm^2) would be needed to achieve a similar surface excitation. Subsequent interactions with a species being deposited would likewise be affected.

Consequently, we have clearly demonstrated that lasers can be used to control surface charge in both metals and semiconductors. This charge can be very effective in controlling both the rate and type of deposition. However, in addition to controlling the deposition process with a laser, we are also interested in controlling the circuit geometry of the deposition, as discussed below in Part B.

B. Lithography

In the above Part A, we have shown how a laser can be used in the deposition process. Both the deposition rate and type of adspecies can be effectively controlled by using the laser to manipulate surface charge. To build a microelectronic circuit, however, we must also be able to control the position of the deposition.

The geometric layout of the circuit can be controlled in the deposition process by limiting the focus of the laser to a given area. Only this region of the surface will develop an excess (or deficient) surface charge. Thus the adsorption of the chosen circuit component would be selectively favored (or disfavored) in the region.

Once the first layer of the circuit is established, the surface will now be divided into different regimes, e.g., p-doped and n-doped regions. Since the electronic energy levels of each of these regions are different, a laser could be used to selectively excite one region while leaving the neighboring areas unaffected. The adsorption of the next layer of the circuit would consequently be controlled by this regional adjustment of surface charge.

Using the method of localized excitation of the surface would permit one to construct virtually any semiconductor device. However, it would have to be done stepwise, where each circiut component is built bit by bit across the surface. This could prove to be very time consuming for large circuits.

Over the past several years, a number of researchers[58] have observed periodic patterns developing on the surfaces of solids that were exposed to laser radiation. These patterns have been seen on various metals, insulators, and both doped and pure semiconductors. Since many IC, like charge-coupled devices and memory chips, have a large degree of order in their surface design, using the laser-induced periodic surface structure as a means to create circuits is a distinct possibility.

To resolve any difficulties in the creation of microelectronic circuits by this method, one must consider how this laser-induced periodic surface structure is produced. Incident radiation of the laser is converted to surface plasmons via surface roughness. These surface plasmons in turn create a periodic electric field on the surface.[59] This field in turn leads to selective enhancement of the deposition process. Brueck and Ehrlich[60] have adapted the formalism of Rayleigh[61] to describe this

phenomenon. They have found that the growth rate of the patterns is proportional to the laser intensity. However, their theory is perturbative and only can be used to explain how the periodic structure is initiated.

Recently[62] there has appeared a solution of the problem of a square-well metallic grating in an applied electromagnetic field (Figure 7b). Such a solution is restricted to explaining the most qualitative features of sinusoidal grating formation. We have established a general formulation of the problem which is capable in principle of handling gratings of any shape or depth.[63]

For p-wave scattering, Maxwell's equations can be written as

$$\frac{\partial^2 H_y}{\partial z^2} + \frac{\partial^2 H_y}{\partial x^2} + \epsilon(x)k_0^2 H_y = \frac{\partial H_y}{\partial x} \frac{\partial}{\partial x} [\ln\epsilon(x)], \tag{46}$$

where H_y is the component of the magnetic field H in the direction perpendicular to the lattice vector of the grating (Figure 7). For a square-well grating, H_y is separable,

$$H_y(x,y) = Z(z)X(x), \tag{47}$$

and Eq. (46) can be written as two coupled first-order differential equations:

$$\frac{\partial Z^2}{\partial z^2} = -\Lambda^2 z \tag{48a}$$

$$\frac{\partial^2 X}{\partial x^2} - \frac{\partial}{\partial x} [\ln\epsilon(x)] \frac{\partial X}{\partial x} + [\epsilon(x)k_0^2 - \Lambda^2]X = 0. \tag{49a}$$

When the applied radiation is incident normal to the grating, it is found that Λ is the solution of the equation

$$1 - \cos(\beta d/2)\cos(\alpha d/2) + 1/2[\varepsilon\alpha/\beta + \beta/(\alpha\varepsilon)]\sin(\beta d/2)\sin(\alpha d/2) = 0, \qquad (50)$$

where d is the period of the grating, ε is the dielectric constant of the grating, $\alpha = (k_0^2 - \Lambda^2)^{1/2}$ and $\beta = (\varepsilon k_0^2 - \Lambda^2)^{1/2}$.

The problem to be considered (Figure 7c) is that of a multilayered grating. In each layer the grating is periodic and the general solution to Eq. (48) for the n-th layer may be written as

$$\psi_n^{II} = \sum_\ell X_{n\ell}(x)[A_{n\ell}e^{i\Lambda_{n\ell}z} + B_{n\ell}e^{-i\Lambda_{n\ell}z}], \qquad (51)$$

where the coefficients A and B are to be determined by the boundary conditions between layers, and $\Lambda_{n\ell}$ is the ℓ-th solution to Eq. (50) for the n-th layer. By applying the boundary condition of continuity of H_y and $\frac{\partial}{\partial z}$ between layers, we can establish the recursion relations for A and B,

$$\vec{A}_n = E_{n,n-1}\vec{A}_{n-1} + F_{n,n-1}\vec{B}_{n-1} \qquad (52a)$$

$$\vec{B}_n = C_{n,n-1}\vec{A}_{n-1}, \; +D_{n,n-1}\vec{B}_{n-1}, \qquad (52b)$$

where the matrices C, D, E F are determined by the periodic structure of each layer. Furthermore, we can establish boundary conditions between the top two layers and the two lowest layers. In the topmost (inifinte) layer, the eigensolution is written as[62]

$$\psi^I = e^{-ik_0 z} + \sum_{n=-\infty}^{\infty} R_n e^{ik_0[\gamma_n x + (1-\gamma_n^2)^{1/2}z]}. \qquad (53)$$

In the lowest (infinite layer) we have

$$\psi^{III} = \sum_{n=-\infty}^{\infty} T_n \, e^{ik_0[\gamma_n x - (\epsilon - \gamma_n^2)^{1/2} z]}, \tag{54}$$

where $\gamma_n = \dfrac{n\lambda}{d}$.

It is now possible to establish

$$\vec{A}_1 = a\vec{D} + b\vec{R} \tag{55a}$$

$$\vec{B}_1 = b\vec{D} + a\vec{R}, \tag{55b}$$

where $\vec{D}$ is a unit vector. In addition,

$$\vec{A}_N = L\vec{B}_N, \tag{56}$$

where N labels the penultimate (finite) layer, and the matrix L is determined by the parameters which characterize that layer. However, by applying the recursion relations of Eq. (52), it is possible to establish

$$\vec{A}_N = J_1 \vec{D} + J_2 \vec{R} \tag{57a}$$

$$\vec{B}_N = K_1 \vec{D} + K_2 \vec{R}. \tag{57b}$$

Rearranging (56) and (57) gives

$$\vec{R} = (J_2 - LK_2)^{-1} (LK_1 - J_1)\vec{D}, \tag{58}$$

and by employing Eq. (52) once more we arrive finally at a matrix equation for the vectors $\vec{A}_M$ and $\vec{B}_M$,

$$\begin{pmatrix} \vec{A}_M \\ \vec{B}_M \end{pmatrix} = \prod_{n=2}^{M} \begin{pmatrix} E_{n,n-1} & F_{n,n-1} \\ C_{n,n-1} & D_{n,n-1} \end{pmatrix} \begin{pmatrix} a & b \\ b & a \end{pmatrix} \begin{pmatrix} \vec{D} \\ \vec{R} \end{pmatrix}.$$

(59)

Preliminary calculations for a square-well cadmium grating have been performed.[63] It was discovered that the perturbation model is in qualitative agreement with this calculation, at least up to grating depths of 50 nm. However, our model for a layered grating is more able to predict qualitatively the behavior of the laser periodic surface deposition at large pattern depths.

Although further work is needed in this area, laser-induced periodic surface deposition holds promise for use in the creation of highly periodic IC. Furthermore, the construction of the metal interconnection grid on the circuit may also be approached through this method.[45] Several other uses for surface waves excited by laser radiation in the circuit lithographic process are possible. For example, if deposited atoms spread from the desired regions into adjacent areas, it may be possible to move them back with a surface wave. Such laser-induced migration has been shown to produce selective motion of adspecies that is several orders of magnitude greater than the typical thermal process.[64] Also, it may be possible to use a surface wave as one of the reference waves in a holographic process. Such a hologram could preserve the entire details of a microelectronic circuit with resolution on the submicrometer level.[65]

Both selectively exciting surface areas and the use of surface waves have been shown to be useful in microelectronic lithography. Laser-induced

periodic pattern deposition, in particular, holds great promise for circuit construction. This technique is, however, in the developmental stage.

C. Annealing and Testing

During the construction of a microelectronic circuit, the semiconductor chip goes through a variety of stresses. These stresses, such as the impact of ion implantation, introduce various types of defects into the crystalline semiconductor material.[66,67] Another problem is the fact that many of the dopant adspecies that were deposited on the surface have failed to penetrate the surface to any significant degree. Such diffusion is necessary to ensure uniform doping of "p" and "n" semiconducting regions. Both of the above problems have been previously solved by heat curing.

The entire semiconductor wafer spends a long time in a high-temperature furnace. This will indeed remove most of the crystal defects caused by fabrication and insure proper diffusion of the dopants. However, the lengthly heating time makes the chip vulnerable to defects introduced by contaminants from the furnace. Furthermore, the heating itself can introduce stresses and defects into the material.

Instead of such oven processing of the semiconductor, many manufacturers are turning to the laser for annealing the surface.[68,69] Laser focusing limits irradiation to specific surface areas, thus minimizing damage to the bulk and the remaining parts of the surface. Furthermore, since the laser exposure is confined to short periods of time on the surface, only the surface states are appreciably excited. Thus, only the ambient temperature of the surface rises; the bulk of the crystal remains untouched. Consequently, this laser "cold" processing[69] ensures no thermal damage to most of the crystal.

In addition to correcting circuit errors by laser annealing, the
selectivity of the laser beam can be used to correct specific mistakes.
In the construction of the metal pathways that link the various regions
of the semiconductor, some connections may be omitted while other extra
connections can be added. This problem may result from faulty design
or damage in the chip fabrication. Experimental work,[70] however, has shown
that a laser can be used to make or break the "metallization" paths. Conse-
quently, the laser proves itself useful in correcting both crystal defects
and specific circuit problems.

Finally, the laser can be used to monitor semiconductor crystal growth
and sense defects in the IC.[71] In the growth of crystal, the laser can
monitor the appearance of defects in the cyrstalline structure. Consequently,
the conditions of growth can then be immediately altered to minimize these
defects. Furthermore, after the circuit is etched on the semiconductor
chip, the laser light can be scattered off the chip and the signal compared
with a standard. Such laser inspection is much faster and more error free
than visual inspection with an optical microscope.

IV. Concluding Remarks

Lasers clearly play an important role in heterogeneous catalysis. We
have shown them to be effective in the control of the rate and specificity
of both desorption and migration. Surface chemical reactions can also be
effectively stimulated by exposure to laser radiation. The results so far
indicate the possible realization of synergistic catalysis with a combined
laser-surface system, which could be more efficient than the laser or the
surface alone. In the realm of microelectronics, the laser has been

demonstrated to not only increase the deposition of a new circuit layer but to selectively regulate the lithographic pattern of the circuit. The laser has also been shown to be a major boom to the electronics industry in the annealing and final testing of integrated circuits. Finally, further work is suggested in the area of laser-stimulated patterned deposition for the duplication of present circuits by holography and the construction of highly-ordered microelectronic chips.

Figure Captions

1. Schematic potential energy curves as functions of the normal distance z
   from the substrate surface. The incoming particle with an initial
   kinetic energy K_j may be adsorbed onto the surface by the transition
   from the electronic state I to state II'. The curve-crossing proba-
   bility may be enhanced by a visible laser (frequency ω_{L1}) inducing
   electronic excitation of state II to II', and an IR laser (frequency
   ω_{L2}) inducing vibrational excitation within the bound states of the
   diabatic potential curve II'. The most probable transition occurs
   at the crossing point X_c.

2. Schematic diagrams of adspecies-surface systems and the associated energy
   levels, where A, B and M represent the adspecies (adatom or admolecule),
   C represents the substrate (or bath modes), and the laser radiation is
   indicated by the wiggly lines. Several types of desorption channels are
   illustrated: (I) direct desorption via active-mode excitation, (II) direct
   desorption via the quasi-continuum, (III) indirect desorption via tunneling,
   (IV) indirect desorption via substrate heating, (V) phonon-assisted
   desorption and (VI) indirect desorption via dynamics.

3. Scaling factor S versus $E_A/k_B T_0$ for LCVD via a pyrolytic process, where
   $S = \alpha/W$ as shown in the inset for a Gaussian laser pulse (solid curve).
   The deposition profile is shown by the dashed curve.

4. Dispersion relationship in complex crystal momentum space ($k + i\kappa$) for
   a finite one-dimensional semiconductor. The valence, surface and
   conduction bands are labeled V, S and C, respectively.

5. Absorption cross section, σ (in $\overset{\circ}{A}$), for surface states versus the frequency
   of the exciting radiation.

6. The magnitude of the surface interaction potential (in millihartrees)
   at various distances from the surface. The solid line represents the
   system with excited state $\kappa \simeq -E_g/g$; the dashed line, $\kappa = -0.5\, E_g/g$; and
   the dotted line, $\kappa = -0.1\, E_g/g$, all in the lower surface energy branch.

7. (a) Sinusoidal grating. The hatched area represents the substrate.

    (b) Square-well grating showing a separation into three layers, one
    of which is periodic along the surface, and two of which are uniform.

    (c) Generalization of the square-well grating in which there are
    three periodic layers.

Acknowledgments

Literature Cited

1. Ponec, V; Knor, Z.; Cerny, S. "Adsorption on Solids", CRC Press: Cleveland, Ohio, 1974.

2. Thomas, J.M.; Thomas, W. J. "Introduction to the Principles of Heterogeneous Catalysis", Academic Press: New York, 1967.

3. Chuang, T. J. J. Chem. Phys., 1981, 74, 1453.

4. Winters, H. F.; Coburn, J. W.; Chuang, T. J. J. Vac. Sci. Tech. B, 1983, 1, 469.

5. Beterov, I. M.; Chebotaev, V. P.; Yurchina, N. I.; Yurchin, B. Ya. Sov. J. Quantum Electron., 1978, 8, 1310.

6. (a) Stewart, C. N.; Ehrlich, G. J. Chem. Phys., 1975, 62, 4672; (b) Winters, H. F. J. Chem. Phys., 1976, 64, 3495; ibid., 1975, 62, 2454.

7. Vokenstein, F. F.; Nagaev, V. B. Kinet. Catal., 1981, 22, 602.

8. For a review see: Goodman, F. O.; Wachman, H. Y. "Dynamics of Gas-Surface Scattering", Academic Press: New York, 1976.

9. Landau, L. D.; Lifshitz, E. M. "Mechnaics", Wiley: New York, 1970.

10. Lin, J.; George, T. F. Surf. Sci., 1981, 108, 304.

11. Viswanathan, R.; Burgess, D. R., Jr.; Stair, P. C.; Weitz, E. J. Vac. Sci. Tech., 1982, 20, 605.

12. Lin. J. "Laser-Stimulated Surface Processes and Heterogeneous Catalysis", Ph.D. Thesis: University of Rochester, 1980.

13. Lin, J.; George, T. F. J. Phys. Chem., 1980, 84, 2957.

14. Lin, J.; George, T. F. Phys. Rev. B, 1983, 28, 76.

15. Lin, J. unpublished results.

16. Goodman, F. O. <u>J. Chem. Phys.</u>, 1983, <u>78</u>, 1582.

17. Taglauer, E.; Heiland, W., Eds. "Inelastic Particle-Surface Collisions", Springer: Berlin, 1981.

18. Recent experimental reviews are: (a) Lichtman, D.; Shapiro, S. <u>CRC Crit. Rev. Solid State Mater. Sci.</u>, 1978, <u>8</u>, 93; (b) Chuang, T. J. <u>Surf. Sci. Rep.</u>, 1983, <u>3</u>, 1.

19. Recent theoretical reviews are: (a) George, T. F.; Lin, J.; Beri, A. C.; Murphy, W. C. <u>Prog. Surf. Sci.</u>, 1984, in press; (b) Lin, J.; Hutchinson, M.; George, T. F. In "Advances in Multi-Photon Processes and Spectroscopy", Lin, S. H., Ed.; World Scientific Publishing Co.: Singapore, 1984, in press.

20. Kronauer, P.; Menzel, D. "Adsorption-Desorption Phenomena", Ricea, F., Ed.; Academic Press: New York, 1972.

21. Van Hien, N.; Lichtman, D. <u>Surf. Sci.</u>, 1981, <u>103</u>, 535.

22. Letokhov, V. S.; Moushev, V. G.; Shekalin, S. V. <u>Sov. Phys. JETP</u>, 1981, <u>54</u>, 257.

23. Heidberg, J.; Stein, H.; Riehl, E. <u>Phys. Rev. Lett.</u>, 1982, <u>49</u>, 666; ibid., <u>Surf. Sci.</u>, 1983, <u>126</u>, 183.

24. Mashni, M.; Hess, P. Chem. Phys. Lett., 1981, <u>77</u>, 541; ibid., <u>Appl. Phys. B</u>, 1982, <u>28</u>, 224.

25. (a) Chuang, T. J. <u>J. Chem. Phys.</u>, 1982, <u>76</u>, 3829; (b) Chuang, T. J.; <u>J. Vac. Sci. Tech.</u>, 1982, <u>20</u>, 603; (c) Chuang, T. J.; Seki, H. <u>Phys. Rev. Lett.</u>, 1982, <u>49</u>, 382; (d) Seki, H., Chuang, T. J. <u>Solid State Commun.</u>, 1982, <u>44</u>, 473.

26. Cowin, J. P.; Auerbach, D. J.; Becker, C.; Wharton, L. <u>Surf. Sci.</u>, 1978, <u>78</u>, 545.

27. Wedler, G.; Ruhmann, H. <u>Surf. Sci.</u>, 1982, <u>121</u>, 464.

28. Slutsky, M. S.; George, T. F. <u>Chem. Phys. Lett.</u>, 1978, <u>57</u>, 474; ibid., J. Chem. Phys., 1978, <u>70</u>, 1231.

29. Lin, J.; George, T. F. <u>J. Chem. Phys.</u>, 1980, <u>72</u>, 2554.

30. Jedrzejek, C.; Freed, K. F.; Efrima, S.; Metiu, H. <u>Chem. Phys. Lett.</u>, 1980, <u>74</u>, 43; ibid., <u>Surf. Sci.</u>, 1981, <u>109</u>, 191.

31. Lucas, D.; Ewing, G. E. <u>Chem. Phys.</u>, 1981, <u>58</u>, 385.

32. Gortel, Z. W.; Kreuzer, H. J.; Piercy, P.; Teshima, R. <u>Phys. Rev. B</u>, 1983, <u>27</u>, 5066.

33. Yates, J. T.; Zinck, J. J.; Sheard, S.; Weinberg, W. H. J. Chem. Phys., 1979, 70, 2266.

34. Umstead, M. E.; Talley, L. D.; Tevault, D. W.; Lin, M. C. Opt. Eng., 1980, 19, 94.

35. Panchenkov, G. M.; Lebedev, V. P. "Chemical Kinetics and Catalysis", MIR Publishers: Moscow, 1976, Chap. 10.

36. Lin, J.; George, T. F. Chem. Phys. Lett., 1979, 66, 5.

37. (a) Chandrasekhar, S. Rev. Mod. Phys., 1943, 15, 1; (b) Collins, F. C.; Kimball, G. E. J. Colloid Sci., 1949, 4, 425; (c) Stowell, M. J. Philos. Mag., 1972, 26, 349.

38. (a) Freeman, D. L.; Doll, J. D. J. Chem. Phys., 1983, 78, 6002; ibid., 1983, 79, 2343; (b) Doll, J. D.; Freeman, D. L. Surf. Sci., 1983, 134, 769.

39. Lin, J.; George, T. F. J. Chem. Phys., 1983, 78, 5197.

40. Goldanskii, V. I.; Namoit, V. A.; Khokholov, R. V. Sov. Phys. JETP, 1976, 43, 1226.

41. Karlov, N. V.; Lukyanchuk, B. S. Sov. J. Quantum Electron., 1981, 11, 909.

42. Metiu, H.; Gadzuk, J. W. J. Chem. Phys., 1981, 74, 2641.

43. For recent studies see: Osgood, R. M., Jr.; Brueck, S. R. J., Eds.; "Laser Diagnostics and Photochemical Processing for Semiconductor Devices", Elsevier: New York, 1983. [This is Volume 17 of the Materials Research Society Symposium Proceedings.]

44. Ehrlich, D. J.; Tsao, J. Y. J. Vac. Sci. Tech. B, 1983, 1, 969.

45. Ehrlich, D. J.; Osgood, R. M., Jr.; Deutsch, T. F. IEEE J. Quantum Electron., 1980, QE-16,1233; ibid., Appl. Phys. Lett., 1980, 36, 698.

46. Wood, T. H.; White, J. C.; Thacker, B. A. In Ref. 41, p. 35.

47. Ehrlich, D. J.; Tsao, J. Y. In Ref. 41, p. 3.

48. McWilliams, B. M.; Herman, I. P., Mitlitsky, F.; Hydre, R. A.; Wood, L. L. Appl. Phys. Lett., 1983, 43, 946; ibid. In Ref. 41, p. 9.

49. (a) Tsao, J. Y.; Ehrlich, D. J. In Ref. 41, p. 235; (b) Ehrlich, D. J.; Tsao, J. Y. Appl. Phys. Lett., 1982, 41, 297.

50. Lin, J.; George, T. F. J. Appl. Phys.,1983, 54, 382.

51. Lundqvist, S. In "Surface Science", International Atomic Energy Agency: Viennia, 1975.

52. Murphy, W. C.; George, T. F. Surf. Sci., 1982, 114, 189.

53. Murphy, W. C.; Lee, K.-T.; George, T. F. Surf. Sci., 1983, 127, L156.

54. Murphy, W. C.; Beri, A. C.; George, T. F.; Lin, J. In Ref. 43, p. 273.

55. Murphy. W. C.; George, T. F. J. Phys. Chem., 1982, 86, 4481.

56. George, T. F.; Lam, K.-S.; Hutchinson, M.; Murphy, W. C. In "Advances in Laser Spectroscopy", Vol. 2, Garetz, B. A.; Lombardi, J. R., Eds.; Wiley: New York, 1983.

57. Murphy, W. C.; George, T. F. J. Chem. Phys., 1984, in press.

58. van Driel, H. M.; Sipe, J. E.; Young, J. F. Phys. Rev. Lett., 1982, 49, 1955 and references therein.

59. Sipe, J. E.; Young, J. F.; Preston, J. S.; van Driel, H. M. Phys. Rev. B, 1983, 27, 1141.

60. Brueck, S. R. J.; Ehrlich, D. J. Phys. Rev. Lett., 1982, 48, 1678.

61. Lord Rayleigh Philos. Mag., 1907, 14, 60.

62. Sheng, P.; Stepheman, R. S.; Sanda, P. N. Phys. Rev. B, 1982, 26, 2907.

63. Hutchinson, M.; Lee, K.-T.; Murphy, W. C.; Beri, A. C.; George, T. F. In "Laser-Controlled Chemical Processing of Surfaces", Johnson, A. W.; Ehrlich, D. J., Eds.; Elsevier: New York, in press. [This is Volume 29 of the Materials Research Society Symposium Proceedings.]

64. Murphy, W. C.; Huang, X.-Y.; George, T. F. Chem. Phys. Lett., 1984, 104, 303.

65. Huang, X.-Y., unpublished results.

66. Auston, D. H.; Brown, W. L.; Celler, G. C. Bell Laboratories Record, 1979, July/August, 187.

67. Lyman, J. Electronics, 1977, 50 (15), 81.

68. Mason, B. Electronics, 1979, 52 (5), 90.

69. Kaplan, R. A.; Cohen, M. G.; Kiu, K. C. Electronics, 1980, 53 (4), 137.

70. Brinton, J. B. Electronics, 1981, 54 (8), 39.

71. Waller, L. Electronics, 1980, 53 (21), 46.

X_c
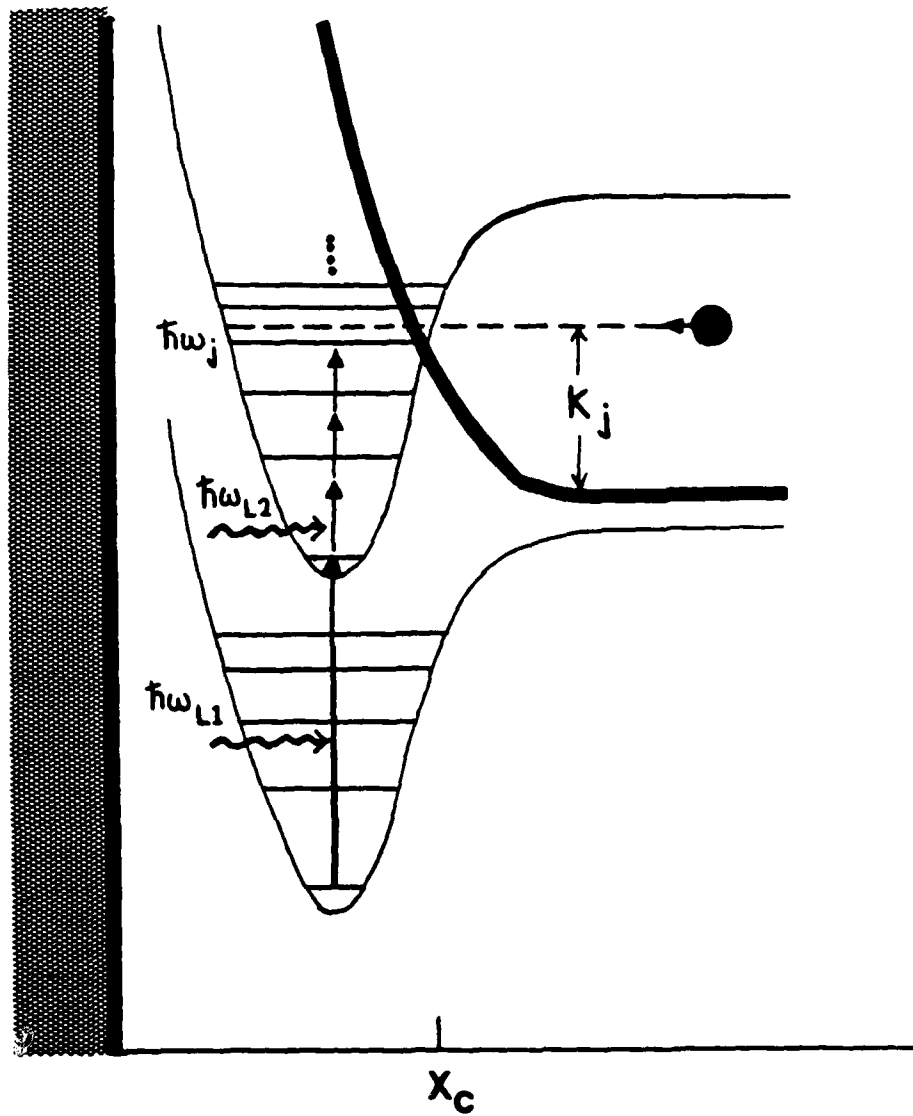
Fig. 1
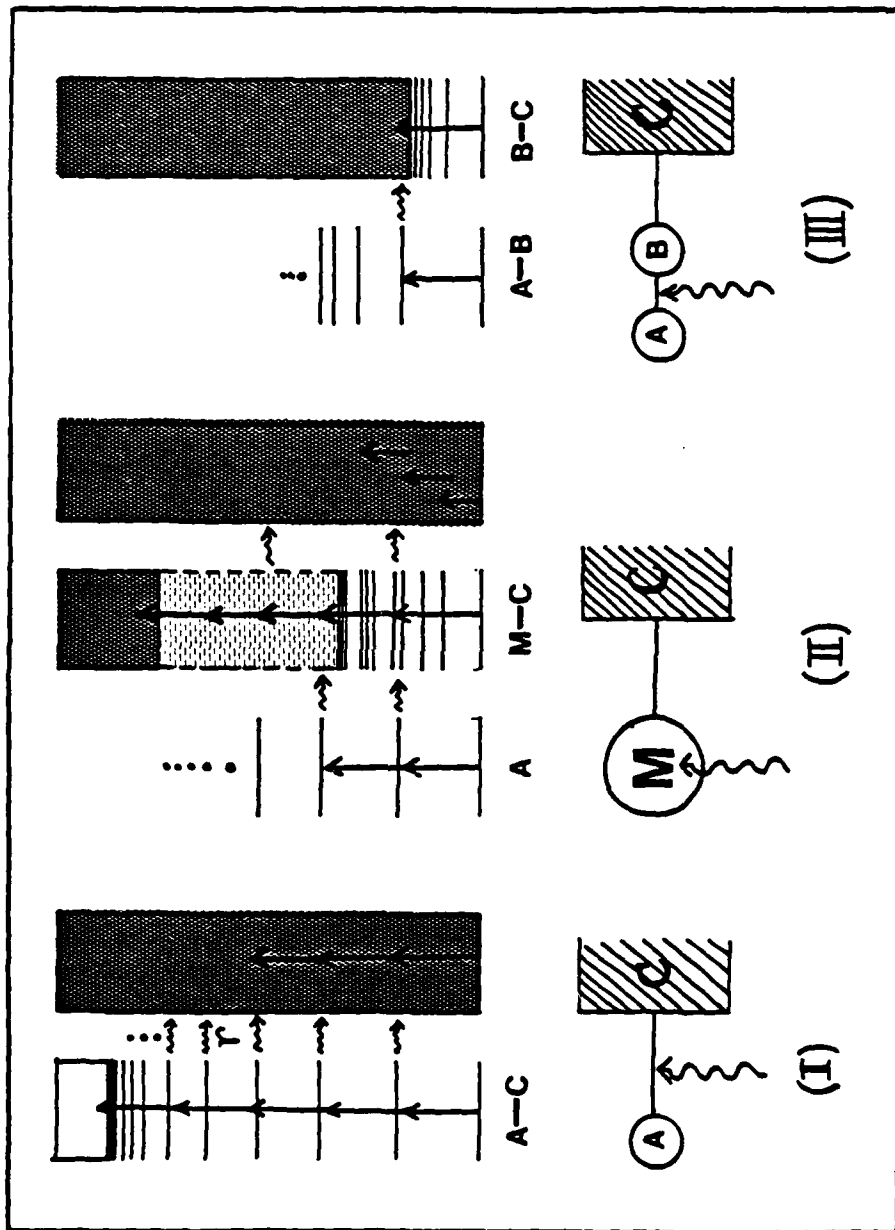
Fig. 2 (I)-(III)
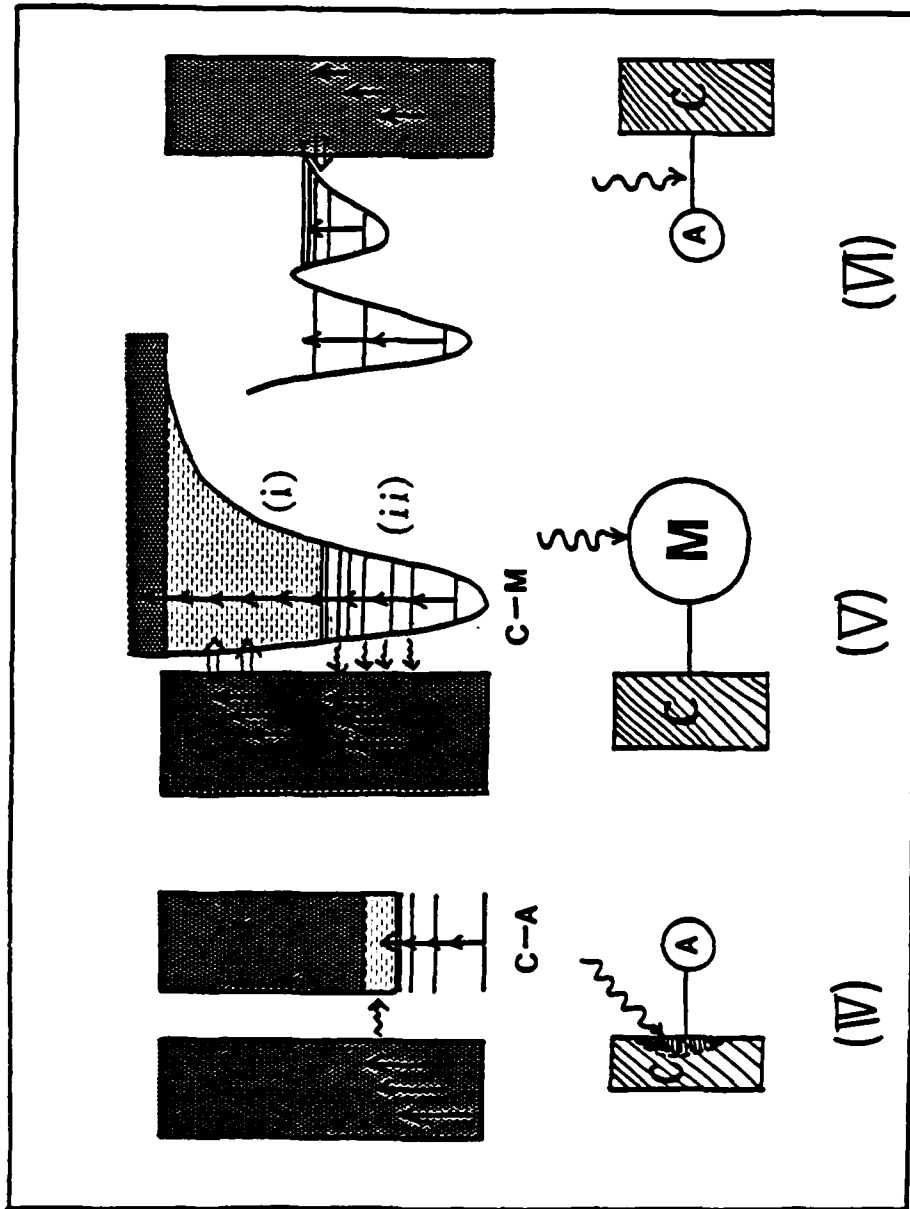
Fig. 2 (Ⅳ)-(Ⅵ)
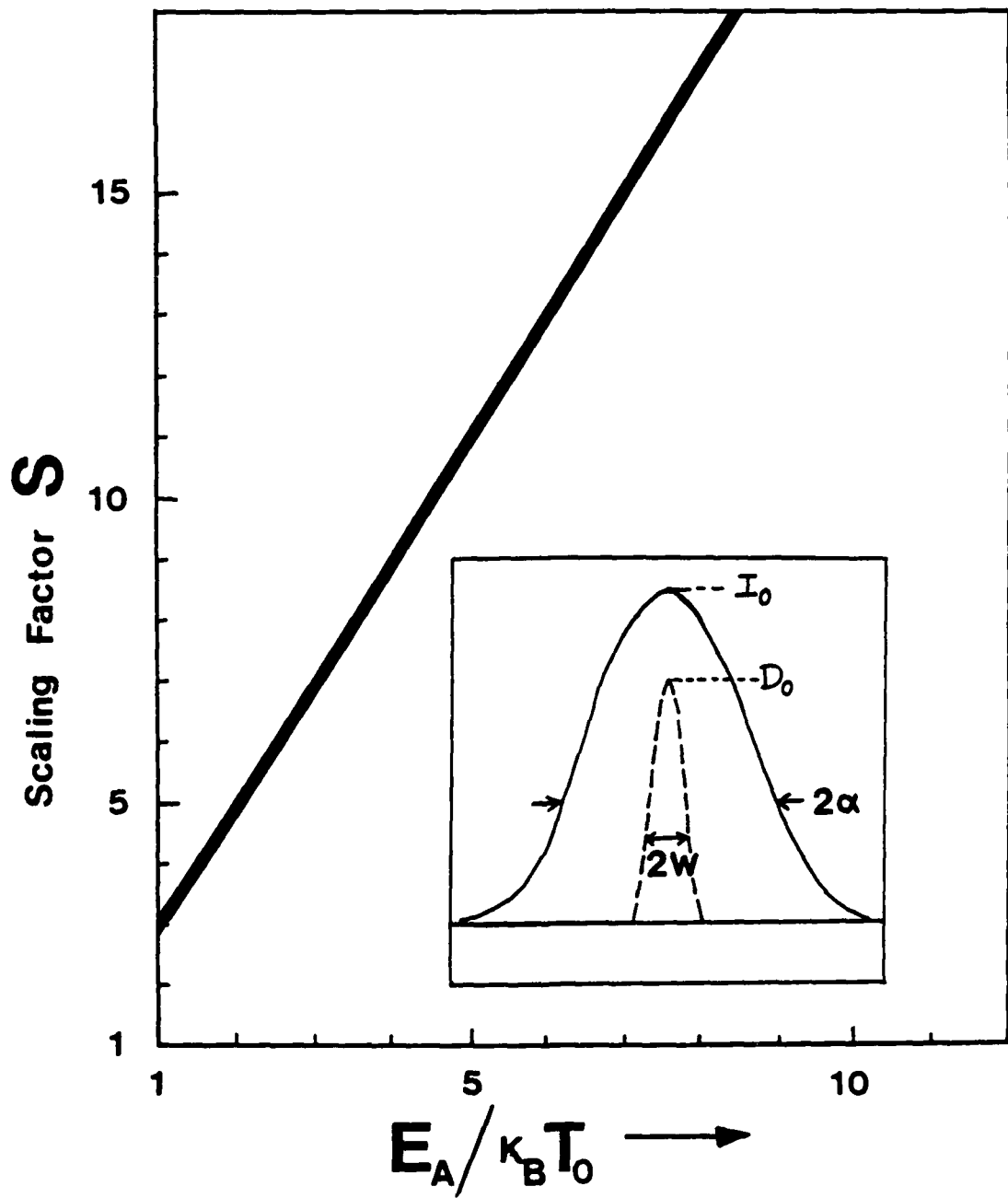
Fig. 3

Fig. 4

Fig. 5

Fig. 6

a

b

Ψ^I

Ψ^{II}

Ψ^{III}

c

Ψ^I

Ψ_1^{II}

Ψ_2^{II}

Ψ_3^{II}

Ψ^{III}
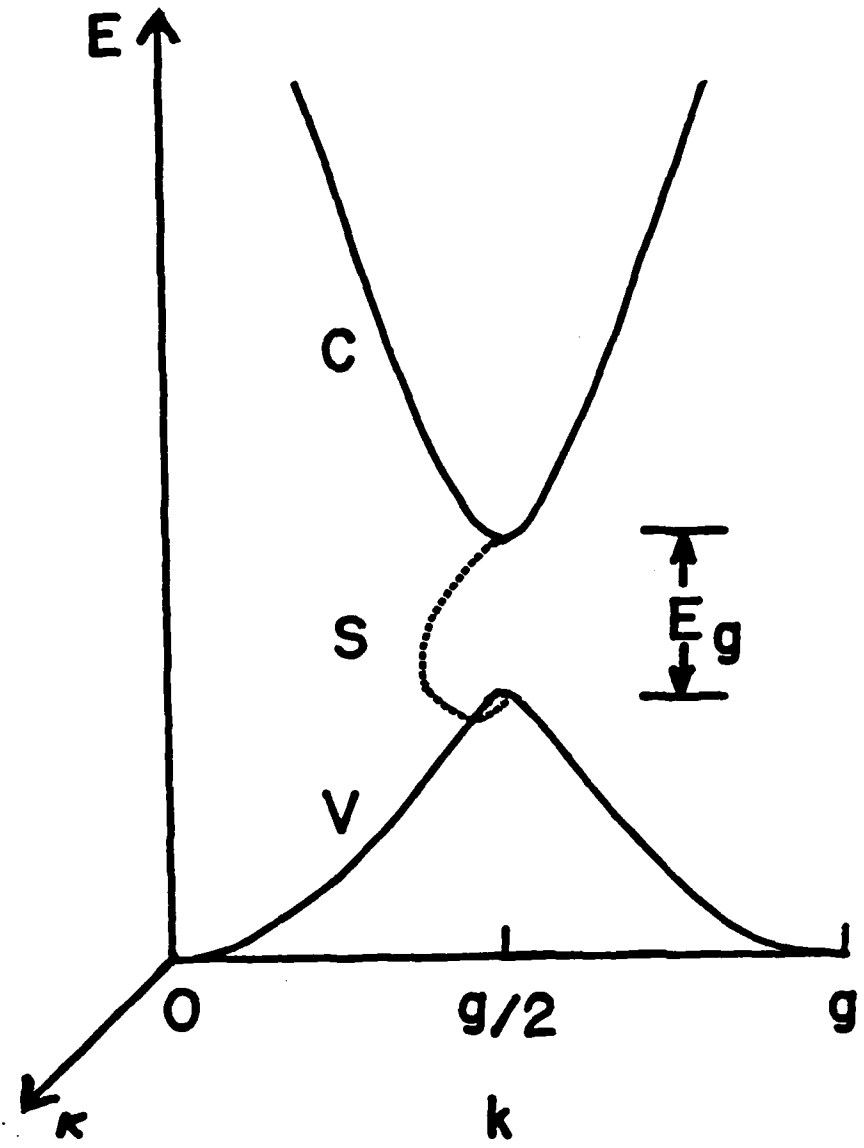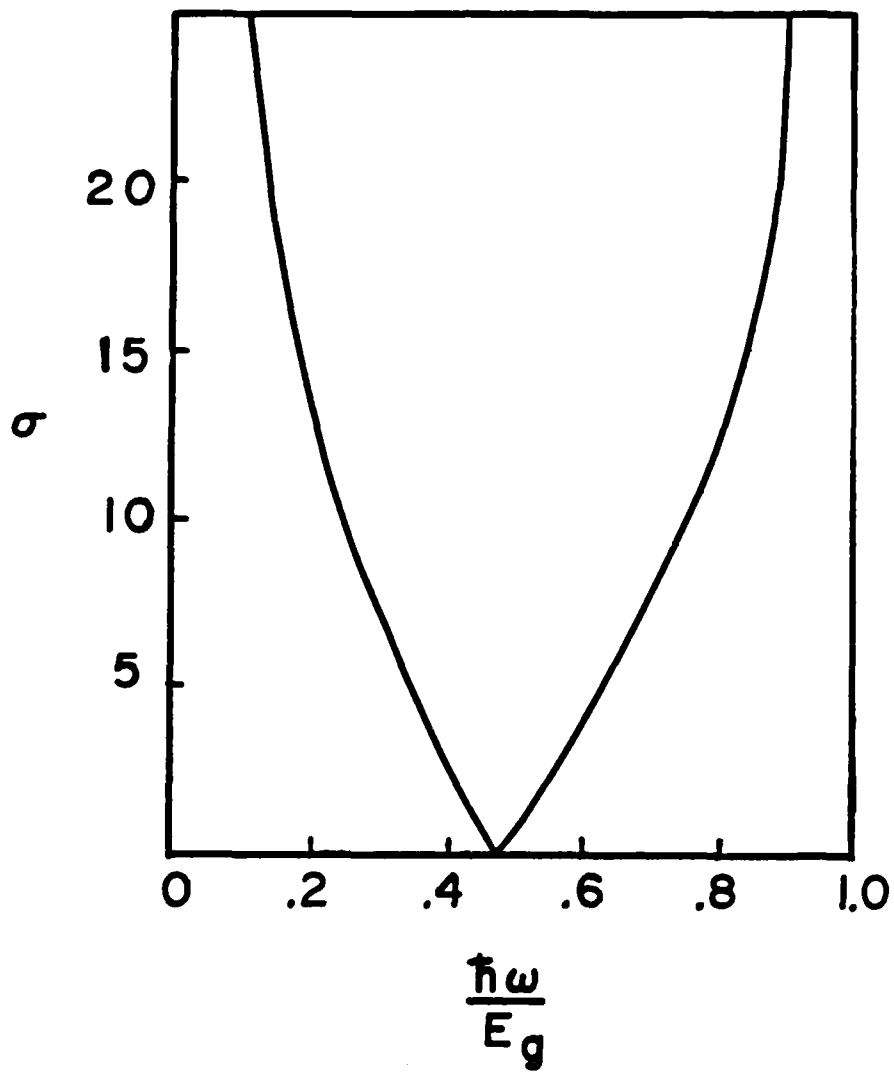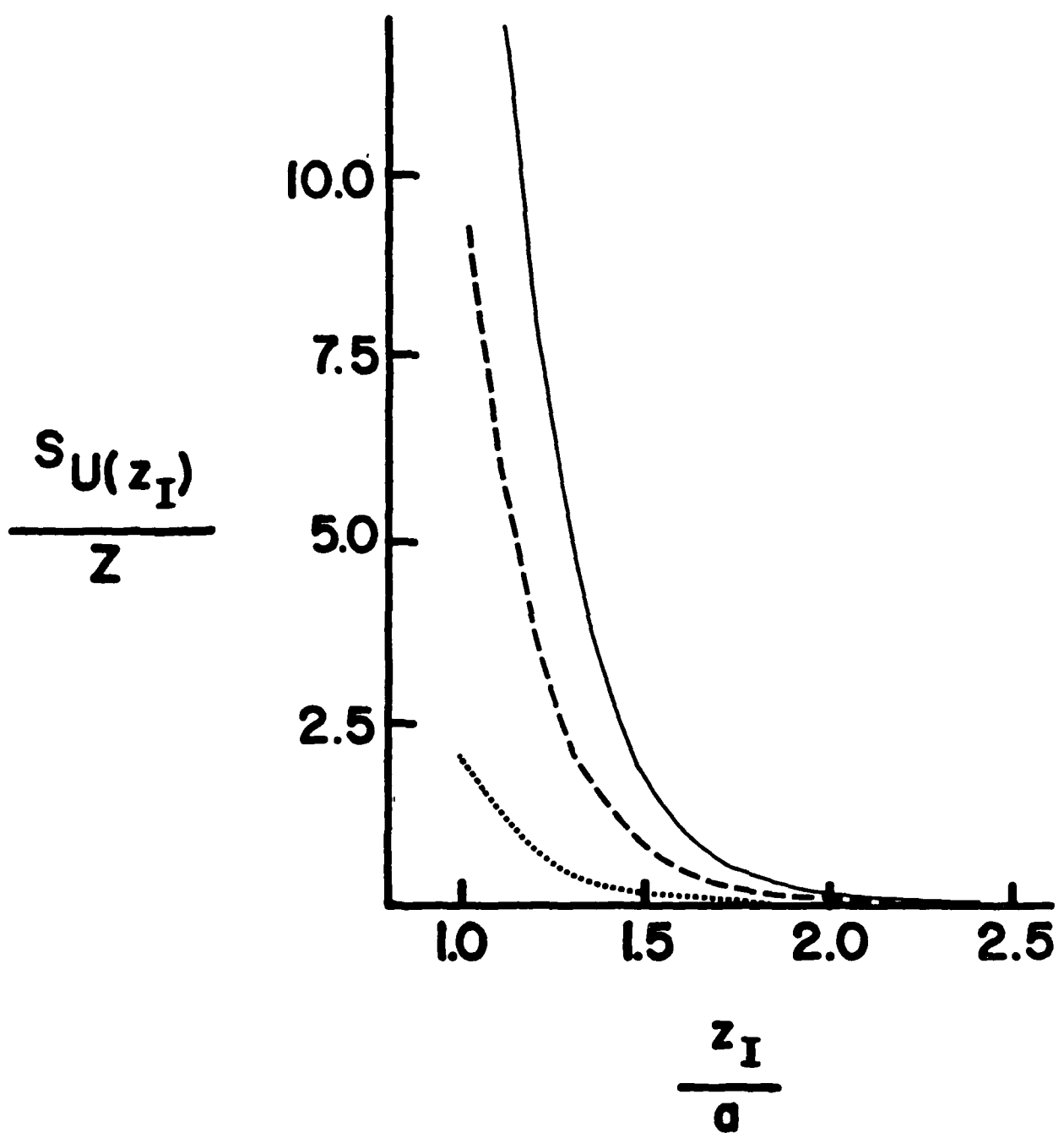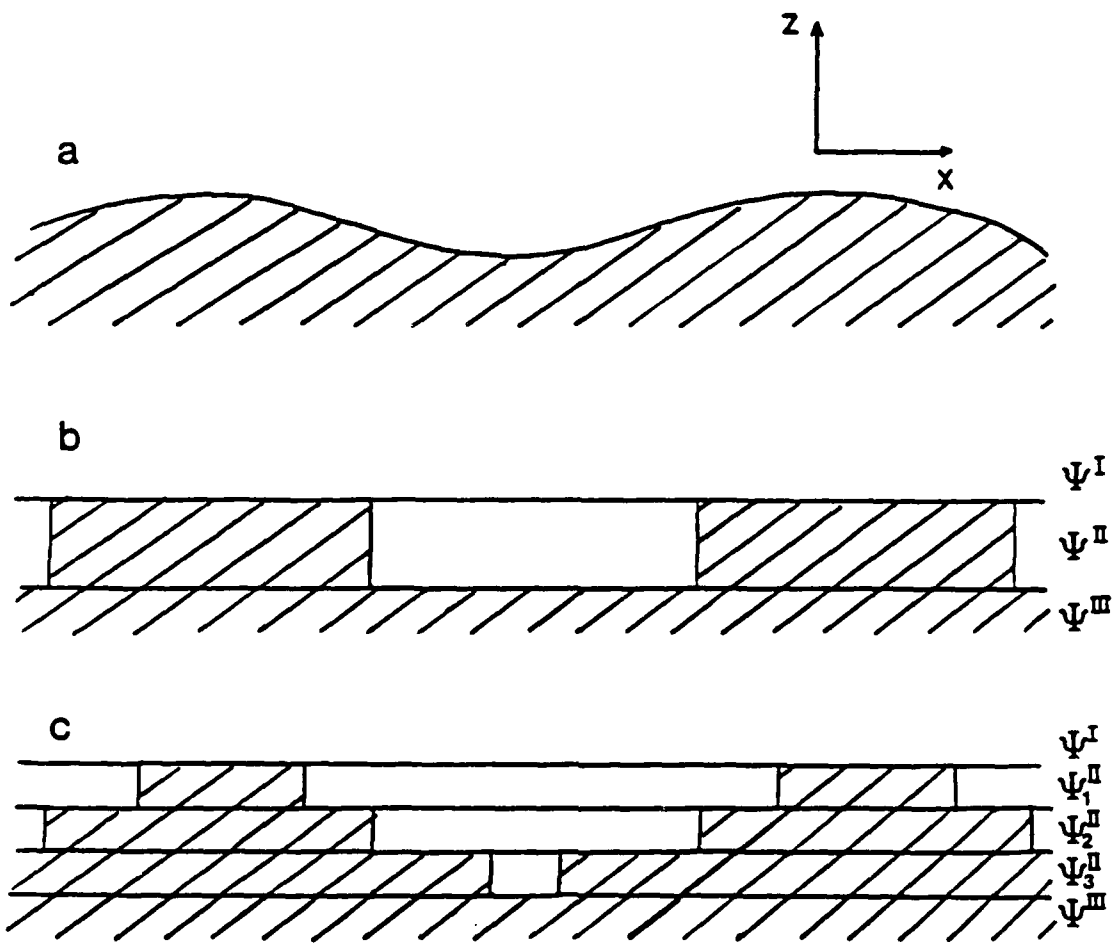
Fig. 7

TECHNICAL REPORT DISTRIBUTION LIST, GEN

	No. Copies		No. Copies
Office of Naval Research Attn: Code 413 800 N. Quincy Street Arlington, Virginia 22217	2	Naval Ocean Systems Center Attn: Technical Library San Diego, California 92152	1
ONR Pasadena Detachment Attn: Dr. R. J. Marcus 1030 East Green Street Pasadena, California 91106	1	Naval Weapons Center Attn: Dr. A. B. Amster Chemistry Division China Lake, California 93555	1
Commander, Naval Air Systems Command Attn: Code 310C (H. Rosenwasser) Washington, D.C. 20360	1	Scientific Advisor Commandant of the Marine Corps Code RD-1 Washington, D.C. 20380	1
Naval Civil Engineering Laboratory Attn: Dr. R. W. Drisko Port Hueneme, California 93401	1	Dean William Tolles Naval Postgraduate School Monterey, California 93940	1
Superintendent Chemistry Division, Code 6100 Naval Research Laboratory Washington, D.C. 20375	1	U.S. Army Research Office Attn: CRD-AA-IP P.O. Box 12211 Research Triangle Park, NC 27709	1
Defense Technical Information Center Building 5, Cameron Station Alexandria, Virginia 22314	12	Mr. Vincent Schaper DTNSRDC Code 2830 Annapolis, Maryland 21402	1
DTNSRDC Attn: Dr. G. Bosmajian Applied Chemistry Division Annapolis, Maryland 21401	1	Mr. John Boyle Materials Branch Naval Ship Engineering Center Philadelphia, Pennsylvania 19112	1
Naval Ocean Systems Center Attn: Dr. S. Yamamoto Marine Sciences Division San Diego, California 91232	1	Mr. A. M. Anzalone Administrative Librarian PLASTEC/ARRADCOM Bldg 3401 Dover, New Jersey 07801	1
Dr. David L. Nelson Chemistry Program Office of Naval Research 800 North Quincy Street Arlington, Virginia 22217	1		

TECHNICAL REPORT DISTRIBUTION LIST, 056

Dr. G. A. Somorjai
Department of Chemistry
University of California
Berkeley, California 94720

Dr. J. Murday
Naval Research Laboratory
Surface Chemistry Division (6170)
455 Overlook Avenue, S.W.
Washington, D.C. 20375

Dr. J. B. Hudson
Materials Division
Rensselaer Polytechnic Institute
Troy, New York 12181

Dr. Theodore E. Madey
Surface Chemistry Section
Department of Commerce
National Bureau of Standards
Washington, D.C. 20234

Dr. Chia-wei Woo
Department of Physics
Northwestern University
Evanston, Illinois 60201

Dr. Robert M. Hexter
Department of Chemistry
University of Minnesota
Minneapolis, Minnesota

Dr. J. E. Demuth
IBM Corporation
Thomas J. Watson Research Center
P.O. Box 218
Yorktown Heights, New York 10598

Dr. M. G. Lagally
Department of Metallurgical
  and Mining Engineering
University of Wisconsin
Madison, Wisconsin 53706

Dr. Adolph B. Amster
Chemistry Division
Naval Weapons Center
China Lake, California 93555

Dr. W. Kohn
Department of Physics
University of California, San Diego
La Jolla, California 92037

Dr. R. L. Park
Director, Center of Materials
  Research
University of Maryland
College Park, Maryland 20742

Dr. W. T. Peria
Electrical Engineering Department
University of Minnesota
Minneapolis, Minnesota 55455

Dr. Keith H. Johnson
Department of Metallurgy and
  Materials Science
Massachusetts Institute of Technology
Cambridge, Massachusetts 02139

Dr. J. M. White
Department of Chemistry
University of Texas
Austin, Texas 78712

Dr. R. P. Van Duyne
Chemistry Department
Northwestern University
Evanston, Illinois 60201

Dr. S. Sibener
Department of Chemistry
James Franck Institute
5640 Ellis Avenue
Chicago, Illinois 60637

Dr. Arold Green
Quantum Surface Dynamics Branch
Code 3817
Naval Weapons Center
China Lake, California 93555

Dr. S. L. Bernasek
Princeton University
Department of Chemistry
Princeton, New Jersey 08544

TECHNICAL REPORT DISTRIBUTION LIST, 056

Dr. F. Carter
Code 6132
Naval Research Laboratory
Washington, D.C. 20375

Dr. Richard Colton
Code 6112
Naval Research Laboratory
Washington, D.C. 20375

Dr. Dan Pierce
National Bureau of Standards
Optical Physics Division
Washington, D.C. 20234

Professor R. Stanley Williams
Department of Chemistry
University of California
Los Angeles, California 90024

Dr. R. P. Messmer
Materials Characterization Lab.
General Electric Company
Schenectady, New York ~~22217~~
                       12301

Dr. Robert Gomer
Department of Chemistry
James Franck Institute
5640 Ellis Avenue
Chicago, Illinois 60637

Dr. Ronald Lee
R301
Naval Surface Weapons Center
White Oak
Silver Spring, Maryland 20910

Dr. Paul Schoen
Code 5570
Naval Research Laboratory
Washington, D.C. 20375

Dr. John T. Yates
Department of Chemistry
University of Pittsburgh
Pittsburgh, Pennsylvania 15260

Dr. Richard Greene
Code 5230
Naval Research Laboratory
Washington, D.C. 20375

Dr. L. Kesmodel
Department of Physics
Indiana University
Bloomington, Indiana 47403

Dr. K. C. Janda
California Institute of Technology
Division of Chemistry and Chemical
   Engineering
Pasadena, California 91125

Professor E. A. Irene
Department of Chemistry
University of North Carolina
Chapel Hill, Northc Carolina 27514

Dr. Adam Heller
Bell Laboratories
Murray Hill, New Jersey 07974

Dr. Martin Fleischmann
Department of Chemistry
Southampton University
Southampton S09 5NH
Hampshire, England

Dr. John W. Wilkins
Cornell University
Laboratory of Atomic and
   Solid State Physics
Ithaca, New York 14853

Dr. Richard Smardzewski
Code 6130
Naval Research Laboratory
Washington, D.C. 20375

TECHNICAL REPORT DISTRIBUTION LIST, 056

Dr. R. G. Wallis
Department of Physics
University of California
Irvine, California 92664

Dr. D. Ramaker
Chemistry Department
George Washington University
Washington, D.C. 20052

Dr. P. Hansma
Physics Department
University of California
Santa Barbara, California 93106

Dr. J. C. Hemminger
Chemistry Department
University of California
Irvine, California 92717

Professor T. F. George
Chemistry Department
University of Rochester
Rochester, New York 14627

Dr. G. Rubloff
IBM
Thomas J. Watson Research Center
P.O. Box 218
Yorktown Heights, New York 10598

Professor Horia Metiu
Chemistry Department
University of California
Santa Barbara, California 93106

Captain Lee Myers
AFOSR/NC
Bollig AFB
Washington, D.C. 20332

Professor Roald Hoffmann
Department of Chemistry
Cornell University
Ithaca, New York 14853

Dr. R. W. Plummer
Department of Physics
University of Pennsylvania
Philadelphia, Pennsylvania 19104

Dr. E. Yeager
Department of Chemistry
Case Western Reserve University
Cleveland, Ohio 41106

Professor D. Hercules
University Pittsburgh
Chemistry Department
Pittsburgh, Pennsylvania 15260

Professor N. Winograd
Department of Chemistry
Pennsylvania State University
University Park, Pennsylvania 16802

Dr. G. D. Stein
Mechanical Engineering Department
Northwestern University
Evanston, Illinois 60201

Professor A. Steckl
Department of Electrical and
  Systems Engineering
Rensselaer Polytechnic Institute
Troy, NewYork 12181

Professor G. H. Morrison
Department of Chemistry
Cornell University
Ithaca, New York 14853

Dr. David Squire
Army Research Office
P.O. Box 12211
Research Triangle Park, NC 27709

DATE
ILME